The Type 2 Diabetes–Associated Gene *Ide* Is Required for Insulin Secretion and Suppression of α-Synuclein Levels in β-Cells

Pär Steneberg,[1] Lisandro Bernardo,[1] Sara Edfalk,[1] Lisa Lundberg,[1] Fredrik Backlund,[1] Claes-Göran Östenson,[2] and Helena Edlund[1]

Genome-wide association studies have identified several type 2 diabetes (T2D) risk loci linked to impaired β-cell function. The identity and function of the causal genes in these susceptibility loci remain, however, elusive. The *HHEX/IDE* T2D locus is associated with decreased insulin secretion in response to oral glucose stimulation in humans. Here we have assessed β-cell function in *Ide* knockout (KO) mice. We find that glucose-stimulated insulin secretion (GSIS) is decreased in *Ide* KO mice due to impaired replenishment of the releasable pool of granules and that the *Ide* gene is haploinsufficient. We also show that autophagic flux and microtubule content are reduced in β-cells of *Ide* KO mice. One important cellular role for IDE involves the neutralization of amyloidogenic proteins, and we find that α-synuclein and IDE levels are inversely correlated in β-cells of *Ide* KO mice and T2D patients. Moreover, we provide evidence that both gain and loss of function of α-synuclein in β-cells in vivo impair not only GSIS but also autophagy. Together, these data identify the *Ide* gene as a regulator of GSIS, suggest a molecular mechanism for β-cell degeneration as a consequence of *Ide* deficiency, and corroborate and extend a previously established important role for α-synuclein in β-cell function. ***Diabetes*** **62:2004–2014, 2013**

Genome-wide association studies have emphasized a key role of β-cell function in type 2 diabetes (T2D) (1–3). The identity and function of the causal genes in these susceptibility loci remain, however, largely unknown. One such locus is positioned in the *HHEX/IDE* gene region (2–4), which in humans is associated with lower 30-min oral glucose-stimulated insulin levels (5,6). The *Ide* gene encodes a multifunctional protein implicated in a diverse set of processes, including development, cell growth and differentiation, proteasome activity, steroid-mediated signaling, and protein degradation (7). An important protective cellular function for IDE is to, via degradation or the formation of stable, irreversible complexes, limit intracellular levels of aggregate prone, amyloidogenic proteins and peptides, thereby preventing formation of toxic oligomers (7,8). *Ide* knockout (KO) mice have been reported to be glucose intolerant and hyperinsulinemic, which was suggested to be the result of reduced insulin degradation and peripheral insulin resistance (9,10). In contrast, Miller et al. (11) reported that blood glucose and insulin levels were normal in fasted-refed *Ide* KO mice.

Here, we have assessed β-cell function in mice lacking the *Ide* gene. We show that insulin secretion is impaired and that islet autophagic flux and microtubule content are reduced in *Ide* KO mice. We also find that IDE can form stable complexes with α-synuclein and that levels of α-synuclein are increased in *Ide* KO islets. Moreover, we find that decreased IDE levels are associated with increased levels of α-synuclein in human T2D islets and that increased expression of α-synuclein in β-cells of normal mice impairs glucose-stimulated insulin secretion (GSIS) and autophagic flux. Thus, our data suggest that *IDE* is a T2D risk gene, causing decreased GSIS and reduced autophagy via impaired suppression of α-synuclein levels in β-cells. These findings suggest that increasing IDE activity and/or expression may represent a therapeutic strategy for treatment of human T2D.

RESEARCH DESIGN AND METHODS

Strains. The animal studies were approved by the Institutional Animal Care and Use Committee of Umeå University and conducted in accordance with Guidelines for the Care and Use of Laboratory Animals. The *Ide* Hz mice (C57BL/6albino:129SvEvBrd mixed background) were generated by Lexicon Genetics (12) and bred to generate *Ide* wild-type (WT) and KO mice, which were then bred independently as previously described (9). The *Snca* KO mice were obtained from the Jackson laboratory (stock 003692). The *Rip/Snca* transgenic construct was generated by cloning a 546-bp, PCR-generated, full-length mouse *Snca* cDNA fragment (primers used: 5′-ctagcccgggatcggagttcttcagaagcctagg-3′ and 5′-ctagcccgggaactgagcacttgtacgccat-3′) behind the *Rip2-hsp68* hybrid promoter (subcloned from Addgene DM#265). Transgenic mice were generated at the Umeå transgene core facility (Umeå University).

Glucose, insulin, and islet amyloid polypeptide/amylin measurements. Glucose tolerance, insulin secretion, and insulin tolerance tests are detailed in the Supplementary Experimental Procedures. Total pancreatic insulin, proinsulin, and islet amyloid polypeptide (IAPP)/amylin from 20-week-old mice were measured using a sensitive rat insulin radioimmunoassay (Linco), rat/mouse proinsulin ELISA kit (Mercodia), and rat/mouse amylin enzyme immunosorbent assay kit (Phoenix Pharmaceuticals), respectively.

Immunohistochemistry, quantification of mRNA, and cell counting. Immunohistochemical staining, quantification of mRNA expression levels, and cell counting were performed essentially as previously described (13,14) and as in the Supplementary Experimental Procedures. The primary and secondary antibodies used for immunohistochemistry and oligonucleotide sequences used for real-time RT-PCR are listed in Supplementary Tables 1 and 2.

In vitro culture of islets. For islet culture experiments, islets were isolated by collagenase perfusion and recovered and equilibrated as previously described (14). In vitro analyses on isolated islets are detailed in the Supplementary Experimental Procedures.

Western blot analyses. Western blot (WB) analyses of isolated mouse and human islets are detailed in the Supplementary Experimental Procedures.

Protein aggregation and degradation assays. Aggregation and degradation assays were performed using recombinant rat-IDE (Calbiochem), human α-synuclein (Prospec), and human insulin (Novo Nordisk) as described in the Supplementary Experimental Procedures.

From the [1]Umeå Center for Molecular Medicine, University of Umeå, Umeå, Sweden; and the [2]Department of Molecular Medicine and Surgery, Endocrinology and Diabetology Unit, Karolinska Institutet, Karolinska University Hospital-Solna, Stockholm, Sweden.
Corresponding author: Helena Edlund, helena.edlund@ucmm.umu.se.
Received 2 August 2012 and accepted 15 January 2013.
DOI: 10.2337/db12-1045
This article contains Supplementary Data online at http://diabetes.diabetesjournals.org/lookup/suppl/doi:10.2337/db12-1045/-/DC1.

Human islets. Human islet studies were approved by the Human Research Ethics Committee of the Karolinska Institute. Human islets were isolated from brain-dead, heart-beating, T2D (n = 4) and nondiabetic multiorgan donors (n = 4) as previously described (15). All donors were in the age range of 48–72 years. The donors with diabetes were on treatment with metformin or insulin. The use of pancreata for scientific purpose was approved in all cases.

Quantification and statistical analyses. Quantification of WB experiments was performed using Image-J software, and all the statistical analyses were performed by heteroscedastic two-tailed Student t test. We considered a value of $P < 0.05$ to be statistically significant.

RESULTS

Glucose intolerance and impaired insulin secretion in *Ide* KO mice. To assess the role of *Ide* in β-cells, we determined GSIS in *Ide*-null mutant mice, denoted *Ide* KO, and *Ide* WT mice. First-phase insulin secretion was modestly reduced and second-phase insulin secretion was severely blunted in *Ide* KO mice (Fig. 1*A*). Consequently, *Ide* KO mice were hyperglycemic (nonfasted glucose levels = 9.9 ± 0.3 mmol/L in *Ide* WT mice and 12.7 ± 0.8 mmol/L in *Ide* KO mice, P = 0.004) and glucose intolerant (Fig. 1*B*). IDE levels are decreased in liver and brain of *Ide* Hz mice (11), and we found a ~30% decrease in IDE levels in *Ide* Hz islets (Fig. 1*C* and *D*). In addition, *Ide* Hz mice showed blunted insulin secretion (Fig. 1*E*) and were glucose intolerant (Fig. 1*F*), providing evidence that the *Ide* gene is haploinsufficient. *Ide* KO mice were not, however, hyperinsulinemic (fasted insulin = 0.39 ± 0.06 ng/mL in *Ide* WT mice and 0.49 ± 0.10 ng/mL in *Ide* KO mice, P = 0.40) and responded to exogenous insulin by reducing glucose levels at a rate identical to that of *Ide* WT mice (Supplementary Fig. 1*A* and *B*).

To further explore the role for *Ide* in β-cell function and to mimic conditions linked to the development of overt diabetes in humans, i.e., insulin resistance, we next analyzed high-fat diet (HFD)–treated and old *Ide* WT and KO mice. Predictably, *Ide* WT mice developed insulin resistance (Supplementary Fig. 1*C* and *D*) and glucose intolerance (Fig. 1*G* and *H*) on HFD and with age, but responded to the developed insulin resistance by enhancing insulin secretion (Fig. 1*I* and *J*). *Ide* KO mice also developed insulin resistance (Supplementary Fig. 1*C* and *D*) on the HFD and with age, but the insulin secretion defect became further pronounced with significantly impaired first- and second-phase insulin secretion (Fig. 1*I* and *J*), manifested as a further deterioration of glucose tolerance where glucose levels actually exceeded the detection limit of the gluconometer, i.e., 33.3 mmol/L, for several of the HFD mice, which therefore had to be counted as 33.3 mmol/L (Fig. 1*G* and *H*). Thus, β-cells of *Ide* KO mice fail to adequately adapt to two of the major triggers of insulin resistance and T2D in humans: obesity and ageing. These findings provide evidence for a role for *Ide* in ensuring GSIS and are consistent with the association of the *HHEX/IDE* susceptibility allele to decreased insulin secretion in humans (5,6,16).

Increased pancreatic insulin and IAPP content in *Ide* KO mice. To examine the underlying cause for the observed insulin secretion defect, we analyzed islet cell number and organization as well as the patterns of expression of the islet hormones insulin, glucagon, somatostatin, and pancreatic polypeptide, glucose transporter type 2 (Glut2), and the transcription factors Ipf1/Pdx1 and Isl1, all of which were normal (Fig. 2*A*–*C*). qRT-PCR analyses revealed that the expression of key β-cell and endocrine transcription factors such as *Isl1*, *Ipf1/Pdx1*, *Nkx6.1*, *NeuroD*, *MafA*, and *Hhex*, as well as that of the kinesin motor protein *Kif11*, which is also part of the *HHEX/IDE* locus (5), was similar in islets of *Ide* WT and *Ide* KO mice (Supplementary Fig. 2*A*). *Ide* KO mice showed a significant increase in pancreatic insulin (~85%) (Fig. 2*D*) and IAPP (~30%) (Fig. 2*E*) content, and confocal microscopy analyses provided evidence of increased density of insulin vesicles (Supplementary Fig. 2*B*). No significant change in glucagon content was observed (data not shown), and the proinsulin/insulin ratio was normal in *Ide* KO islets (Supplementary Fig. 2*C*). Thus, the reduced GSIS observed in *Ide* KO mice does not appear to result from impaired β-cell differentiation, a decreased amount of β-cells, or insufficient insulin content.

Under conditions involving reduced insulin secretion, pancreatic insulin content homeostasis is maintained via induction of autophagy (17,18). The increased insulin and IAPP content of *Ide* KO β-cells suggested that autophagy-mediated maintenance of pancreatic insulin content homeostasis may be reduced. In agreement with this notion, the autophagic marker LC3, the autophagic substrate p62, and polyubiquitinated proteins were accumulated in islets of fasted and fed *Ide* KO mice as compared with those of *Ide* WT mice (Fig. 2*F*, Supplementary Fig. 2*D*, and data not shown). Moreover, LC3 turnover assays (19) showed that, in contrast to *Ide* WT islets, the lysosomal inhibitor chloroquine failed to increase LC3-II levels in starved *Ide* KO islets, and the rate of autophagic flux was reduced by 28% in *Ide* KO islets (Fig. 2*G* and *H*). The expression of key autophagy genes such as *Atg5*, *Atg6/Beclin*, *Atg7*, and *Atg8/LC3* was normal in β-cells of *Ide* KO mice (Supplementary Fig. 2*E*), arguing against a reduced expression of these genes as the underlying cause for the β-cell autophagy defect. Together, these findings indicate that the increased pancreatic insulin and IAPP content of *Ide* KO mice, at least in part, is the consequence of reduced autophagic flux in β-cells of *Ide* KO mice.

Replenishment of the releasable pool of insulin granules is impaired in *Ide* KO mice. To elucidate at what level *Ide* ascertains insulin secretion, we next analyzed the effect of secretagogues on insulin secretion in *Ide* KO and *Ide* WT mice. Glibenclamide, arginine, and carbachol stimulated insulin secretion to the same extent in *Ide* KO and *Ide* WT mice (Fig. 3*A*–*C*). These secretagogues act, however, primarily by stimulating exocytosis of insulin from the releasable pool of granules (20–22), suggesting that docking, priming, and triggering of exocytosis of granules are unimpaired in *Ide* KO mice.

The expression levels of genes involved in glucose uptake, glucose metabolism, and membrane depolarization, i.e., *Glut2*, *glucokinase (GK)*, *SUR1*, and *Kir6.2*, were similar between control and *Ide* KO mice (Supplementary Fig. 3*A*). Control and *Ide* KO islets also showed a similar increase in ATP/ADP ratio in response to glucose (Supplementary Fig. 3*D*), providing evidence that glucose uptake and metabolism are unaffected in β-cells of *Ide* KO mice. The expression of genes involved in exocytosis, such as *Rab3c*, *Rab27a*, *Vamp2*, *Snap25*, *Stx1a*, *Stx4*, *Syt7*, and *Syt9*, was indistinguishable between *Ide* WT and *Ide* KO mice, and there was a nonsignificant tendency to decreased expression of *Rab3b* and increased expression of *Rab3a* in islets of *Ide* KO mice (Supplementary Fig. 3*B* and *C*). Thus, expression of key components of the insulin exocytosis machinery is largely unimpaired in islets of *Ide* KO mice.

To further probe how *Ide* regulates second-phase insulin secretion, we next performed dual arginine stimulation of

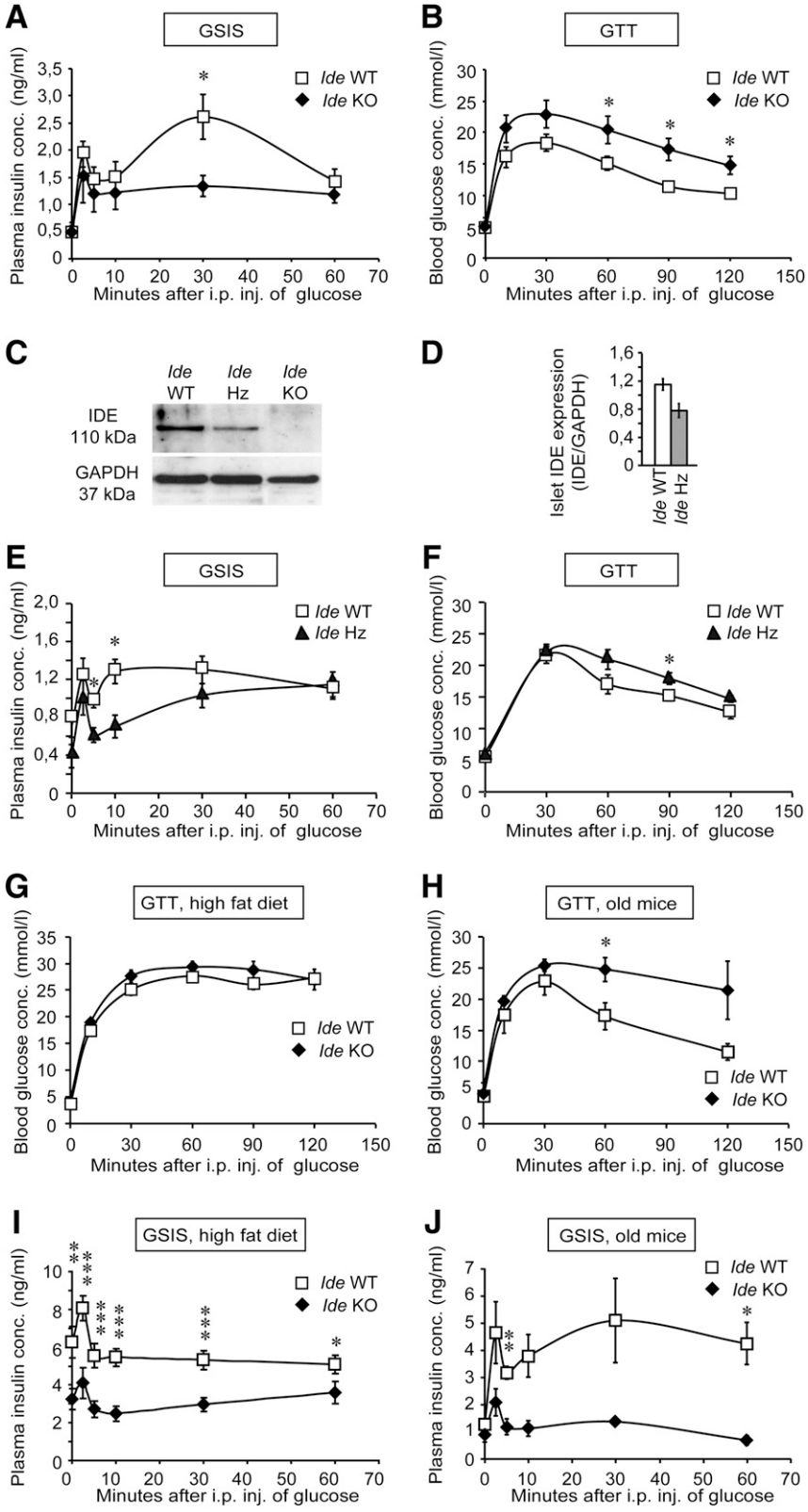

FIG. 1. Impaired insulin secretion and glucose intolerance in *Ide* KO mice. Insulin (*A*) and glucose (*B*) levels during GTT performed on 7–8-week-old *Ide* KO ($n = 8$) and *Ide* WT ($n = 8$) mice. Immunoblot (*C*) and quantification (*D*) analyses of islet IDE expression in *Ide* WT, *Ide* Hz, and *Ide* KO mice ($n = 3$ mice of each genotype). GSIS (*E*) and GTT (*F*) in 20-week-old *Ide* Hz ($n = 7$) and *Ide* WT ($n = 8$) mice. GTT (*G* and *H*) and GSIS (*I* and *J*) on *Ide* KO ($n = 9$) and *Ide* WT mice ($n = 16$) on high-fat diet for 13 weeks (*G* and *I*) and on 12–16-month-old *Ide* KO ($n = 4$) and *Ide* WT mice ($n = 3$) (*H* and *J*). Data are presented as mean ± SEM. *$P < 0.05$; **$P < 0.01$; ***$P < 0.001$ (Student *t* test). GAPDH, glyceraldehyde-3-phosphate dehydrogenase.

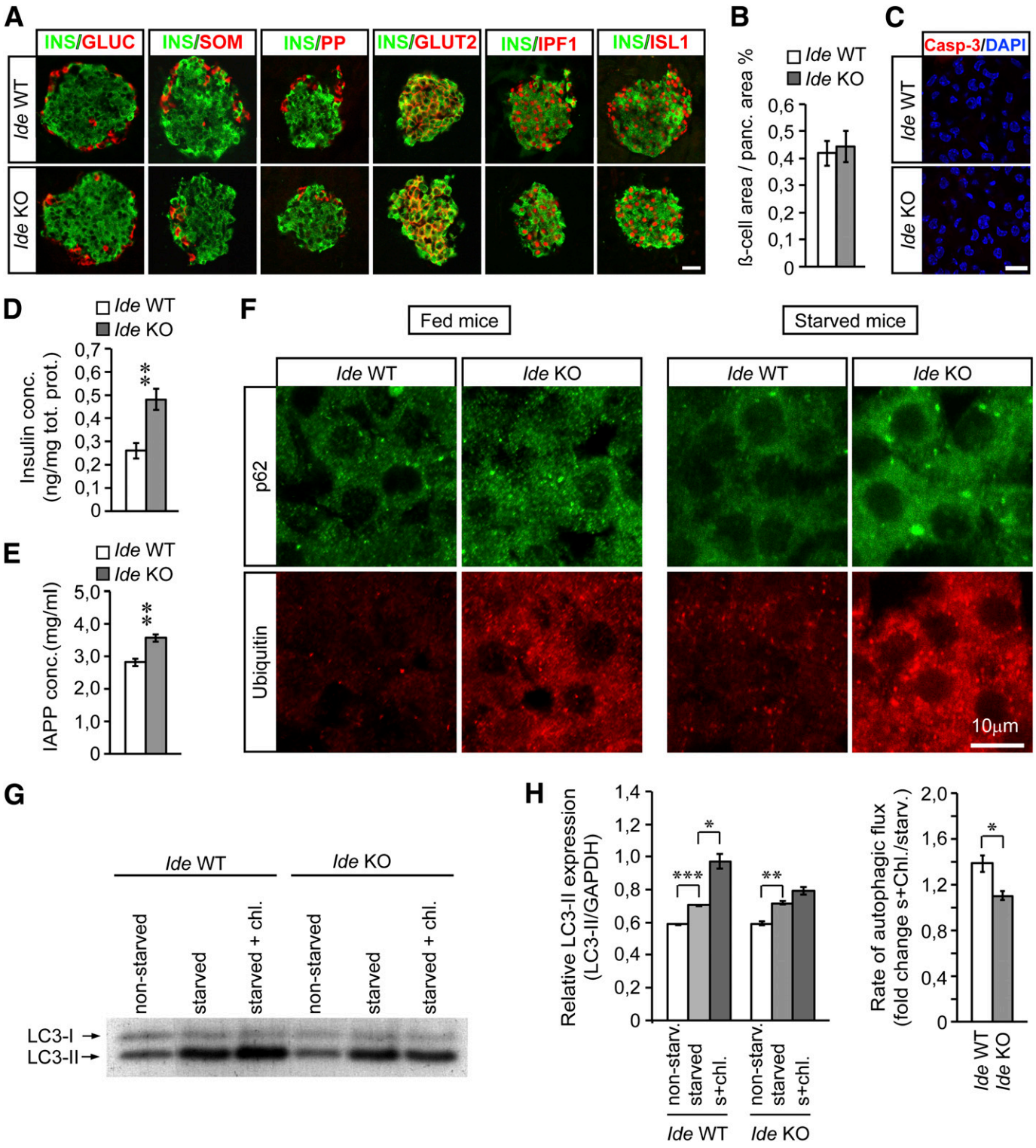

FIG. 2. Increased pancreatic insulin and IAPP content in *Ide* KO mice. *A*: Representative immunohistochemical staining of pancreatic sections from 12-week-old *Ide* KO and *Ide* WT mice showing insulin (green), glucagon, somatostatin, pancreatic polypeptide (PP), Glut2, Ipf1/Pdx1, and Isl1 (all in red). Scale bar, 50 µm. *B*: Quantification of β-cell area in *Ide* WT (n = 3) and *Ide* KO (n = 3) mice. *C*: Representative caspase-3 immunohistochemistry staining of pancreas sections from 14-week-old *Ide* WT and *Ide* KO mice. *D*: Radioimmunoassay analyses of total pancreatic insulin content in *Ide* KO (n = 7) and *Ide* WT mice (n = 4). *E*: Enzyme immunosorbent assay analyses of total pancreatic IAPP content in *Ide* KO (n = 4) and *Ide* WT mice (n = 4). *F*: Representative immunohistochemistry staining of pancreatic sections from fed and 24-h starved *Ide* KO and *Ide* WT mice (n = 3 per genotype) showing p62 and polyubiquitin. Scale bar, 10 µm. *G* and *H*: Immunoblot (*G*) and quantification (*H*) analyses of LC3-II expression in nonstarved and starved *Ide* KO (n = 6 mice) and *Ide* WT (n = 6 mice) islets, in the absence or presence of chloroquine (s + chl). Data are presented as mean ± SEM. *P < 0.05; **P < 0.01; ***P < 0.001 (Student t test). GAPDH, glyceraldehyde-3-phosphate dehydrogenase.

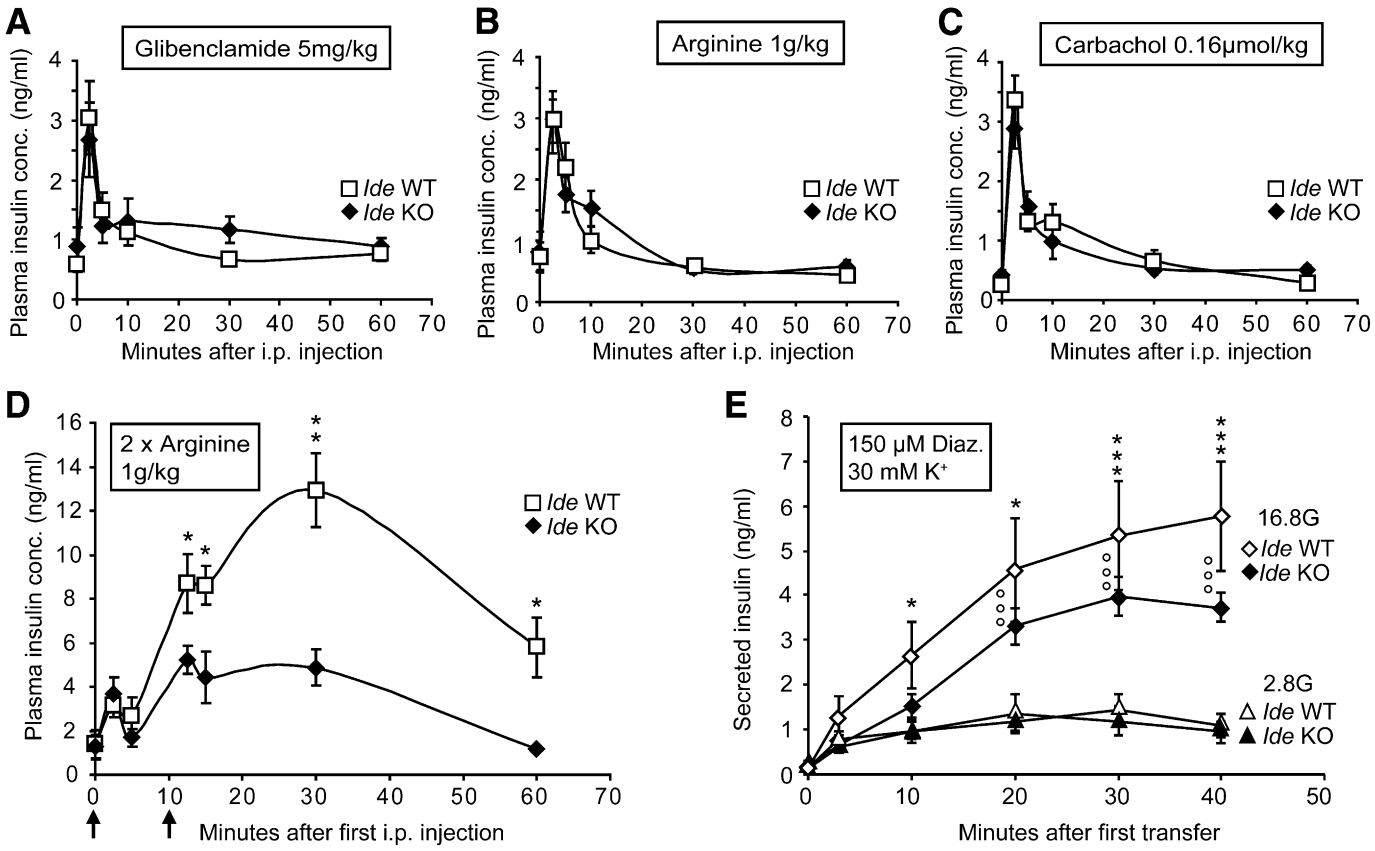

FIG. 3. *Ide* KO mice fail to replenish the readily releasable pool of insulin granules. Insulin secretion after intraperitoneal injection of glibenclamide (12-week-old *Ide* KO [*n* = 7] and *Ide* WT [*n* = 3]) (*A*), arginine (13–17-week-old *Ide* KO [*n* = 11] and *Ide* WT [*n* = 14]) (*B*), and carbachol (14–18-week-old *Ide* KO [*n* = 8] and *Ide* WT [*n* = 9]) (*C*). *D*: Insulin secretion after consecutive, dual arginine injections administered at time 0 and 10 min, indicated by arrows in 16-week-old *Ide* KO (*n* = 6) and *Ide* WT (*n* = 4) mice. *E*: Insulin secretion from four single, size-matched islets incubated in the presence of 150 µmol/L diazoxide and 30 mmol/L K^+ at either 16.8 (diamonds) or 2.8 mmol/L (triangles) glucose. Significance is indicated for comparison of datasets between 16.8 and 2.8 mmol/L glucose for *Ide* WT (*) and *Ide* KO (°), respectively. Islets were isolated from 12–15-week-old Ide KO (*n* = 5) and Ide WT (*n* = 4) mice. Data are presented as mean ± SEM. **P* < 0.05; ***P* < 0.01; */°°°*P* < 0.001 (Student *t* test).**

insulin secretion in vivo with a 10-min interval (23). The first arginine stimulus will empty the releasable pool of granules, and hence the second arginine stimulus will challenge the ability to replenish this pool (23). The insulin secretion response to the first arginine injection was similar in *Ide* WT and *Ide* KO mice, whereas insulin secretion in response to the second arginine stimulus was severely blunted in *Ide* KO mice (Fig. 3*D*). Additionally, in vitro perifusion of isolated islets showed that insulin secretion in response to high (16.8 mmol/L) glucose levels was reduced in *Ide* KO islets (Supplementary Fig. 3*E*). After an intermittent 3-min period of low (2.8 mmol/L) glucose levels, sequential addition of high glucose levels together with glibenclamide was unable to correct the insulin secretion defect in *Ide* KO islets (Supplementary Fig. 3*E*). These findings indicate that recruitment of granules from the reserve pool and/or priming of granules in the releasable pool are decreased in *Ide* KO mice.

The glucose-amplifying pathway contributes to the second phase of insulin secretion by accelerating the priming process of granules (24–26). To investigate the glucose amplifying pathway in *Ide* KO mice, islets were depolarized by high K^+ in the presence of the K_{ATP} channel activator diazoxide. Under these conditions, high glucose (16.8 mmol/L) concentrations generated a robust increase in insulin secretion from both *Ide* WT and *Ide* KO islets, although the relative amount of insulin secreted from *Ide* KO islets was reduced (Fig. 3*E*). Thus, *Ide* KO islets respond to the amplifying pathway of insulin secretion by glucose, indicating that priming of granules is largely unaffected in *Ide* KO β-cells.

Reduced microtubule levels in islets of *Ide* KO mice. The perturbation of insulin granule recruitment as well as autophagy in β-cells of *Ide* KO mice urged us to look for a potential common denominator that might explain these phenotypes. The cytoskeleton and, in particular, microtubules are implicated in efficient insulin granule transport (27), autophagosome formation, transport, and fusion with lysosomes (28,29). Total tubulin was reduced by ~27% in starved *Ide* KO islets compared with *Ide* WT islets (Fig. 4*A* and *B*), and the amount of polymerized tubulin, i.e., microtubules, in starved *Ide* KO islets was ~57% of that observed in *Ide* WT islets (Fig. 4*A* and *B*). Glucose stimulation increases the amount of polymerized tubulin (30), and although both control and *Ide* KO islets increased their levels of polymerized tubulin upon glucose stimulation, total and polymerized tubulin content were still reduced, by ~30%, in glucose-stimulated *Ide* KO islets compared with *Ide* WT islets (Fig. 4*A* and *B*). Glucose stimulation ensures mobilization and trafficking of granules also by inducing the reorganization of F-actin (27). Consequently, F-actin–depolymerizing agents, such as latrunculin B

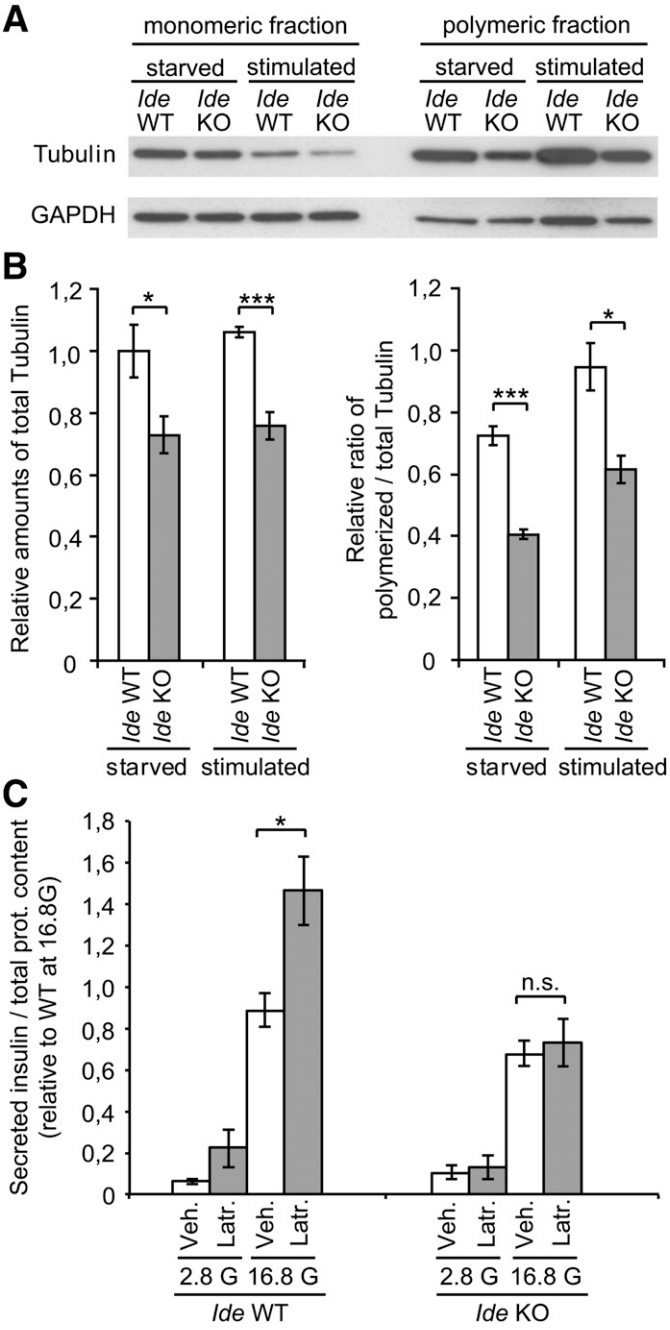

FIG. 4. Microtubule levels are reduced in *Ide* KO islets. Immunoblot (*A*) and quantification (*B*) analyses of monomeric and polymeric tubulin fractions from starved and glucose-stimulated *Ide* KO and *Ide* WT islets (n = 8 mice per genotype). *C*: Insulin secretion from isolated *Ide* KO (n = 4 mice) and *Ide* WT (n = 4 mice) islets after exposure to latrunculin-B at low (2.8 mmol/L) and high (16.8 mmol/L) glucose concentrations. Data are presented as mean ± SEM. *P < 0.05; ***P < 0.001 (Student t test). GAPDH, glyceraldehyde-3-phosphate dehydrogenase; Veh, Vehicle; Latr, Latrunculin B.

(Supplementary Fig. 4*A* and *B*), have been shown to enhance GSIS (27). Phalloidin staining of *Ide* WT and *Ide* KO islets did not, however, reveal any apparent difference in actin organization (Supplementary Fig. 4*C*), and, in contrast to *Ide* WT islets, *Ide* KO islets failed to increase insulin secretion in response to latrunculin B (Fig. 4*C*). These data indicate that the insulin secretion defect of *Ide* KO β-cells is upstream of F-actin reorganization, suggesting that the insulin secretion defect observed in *Ide* KO mice, at least in part, is a consequence of reduced, microtubule-dependent recruitment of granules.

α-Synuclein levels are inversely correlated with IDE levels in islets of *Ide* KO mice and T2D patients. To further assess how loss of IDE activity impairs insulin secretion, autophagy, and tubulin polymerization, we looked for a candidate IDE substrate that would negatively affect these processes. α-Synuclein, encoded by *Snca*, is an amyloidogenic protein negatively correlated with secretion, autophagy, microtubule polymerization, and trafficking (31–34). Moreover, α-synuclein contains the four–amino acid GAXX amyloidogenic region, where X corresponds to amino acids with an aliphatic side chain, which is also present in the IDE substrates amyloidß and IAPP (35). Analyses of α-synuclein protein levels revealed an ~30–40% increase of α-synuclein monomers in *Ide* KO islets compared with *Ide* WT islets and an intermediate (~15%) increase of α-synuclein in *Ide* Hz islets (Fig. 5*A*). Increased levels of α-synuclein were also observed by immunohistochemistry in β-cells of *Ide* KO mice (Fig. 5*B*). These findings suggest that *Ide*, directly or indirectly, regulates α-synuclein levels in β-cells. To further evaluate the impact of increased α-synuclein levels on insulin secretion and autophagic flux, we generated *Rip/Snca* transgenic mice overexpressing α-synuclein in β-cells. *Rip/Snca* mice had blunted GSIS and reduced glucose tolerance (Fig. 5*C*), decreased autophagic flux (~25%) (Fig. 5*D*), and decreased microtubules (~30–40%) (Supplementary Fig. 5*A* and *B*) but normal IDE levels, β-cell numbers, and β-cell turnover (Supplementary Fig. 5*C* and data not shown). Thus, increased levels of α-synuclein in β-cells negatively affect insulin secretion, autophagic flux, and microtubule content.

To explore whether the increased levels of α-synuclein in β-cells of *Ide* KO mice reflect a role for IDE in α-synuclein degradation, recombinant α-synuclein was incubated with recombinant IDE. Although IDE efficiently degraded insulin already within 1 h of incubation, IDE was not capable of degrading α-synuclein even if incubated for 48 h (Fig. 5*E* and data not shown). IDE has also, however, been suggested to function as a "dead-end chaperone" that neutralizes the aggregation of amyloidogenic proteins by forming irreversible, SDS-resistant complexes with monomeric forms of the protein (8). Incubation of α-synuclein alone resulted in the formation of high-molecular-weight complexes corresponding to α-synuclein pentamers and decamers already after 30 min (Fig. 5*E* and Supplementary Fig. 5*D*). Incubation of α-synuclein with IDE not only reduced the formation of these oligomeric complexes but also generated, in a time- and dose-dependent manner, an SDS-resistant, ~130-kDa complex that was recognized by α-synuclein antibodies (Fig. 5*E* and *F* and Supplementary Fig. 5*D*). The ~130-kDa complex corresponds to the combined molecular weight of IDE (~110 kDa) and α-synuclein (~17 kDa on an SDS-PAGE) and was recognized also by IDE antibody (Supplementary Fig. 5*E*). Moreover, IDE antibodies dose-dependently competed with the formation of the ~130-kDa IDE/α-synuclein complex (Supplementary Fig. 5*F*). IDE was not, however, capable of affecting preformed high-molecular-weight α-synuclein oligomers, although the ~130-kDa complex was still generated (Supplementary Fig. 5*G*). These findings indicate that IDE, by complexing with α-synuclein monomers, reduces the formation of α-synuclein oligomers.

We next assessed IDE and α-synuclein protein levels in islets isolated from T2D patients and nondiabetic controls.

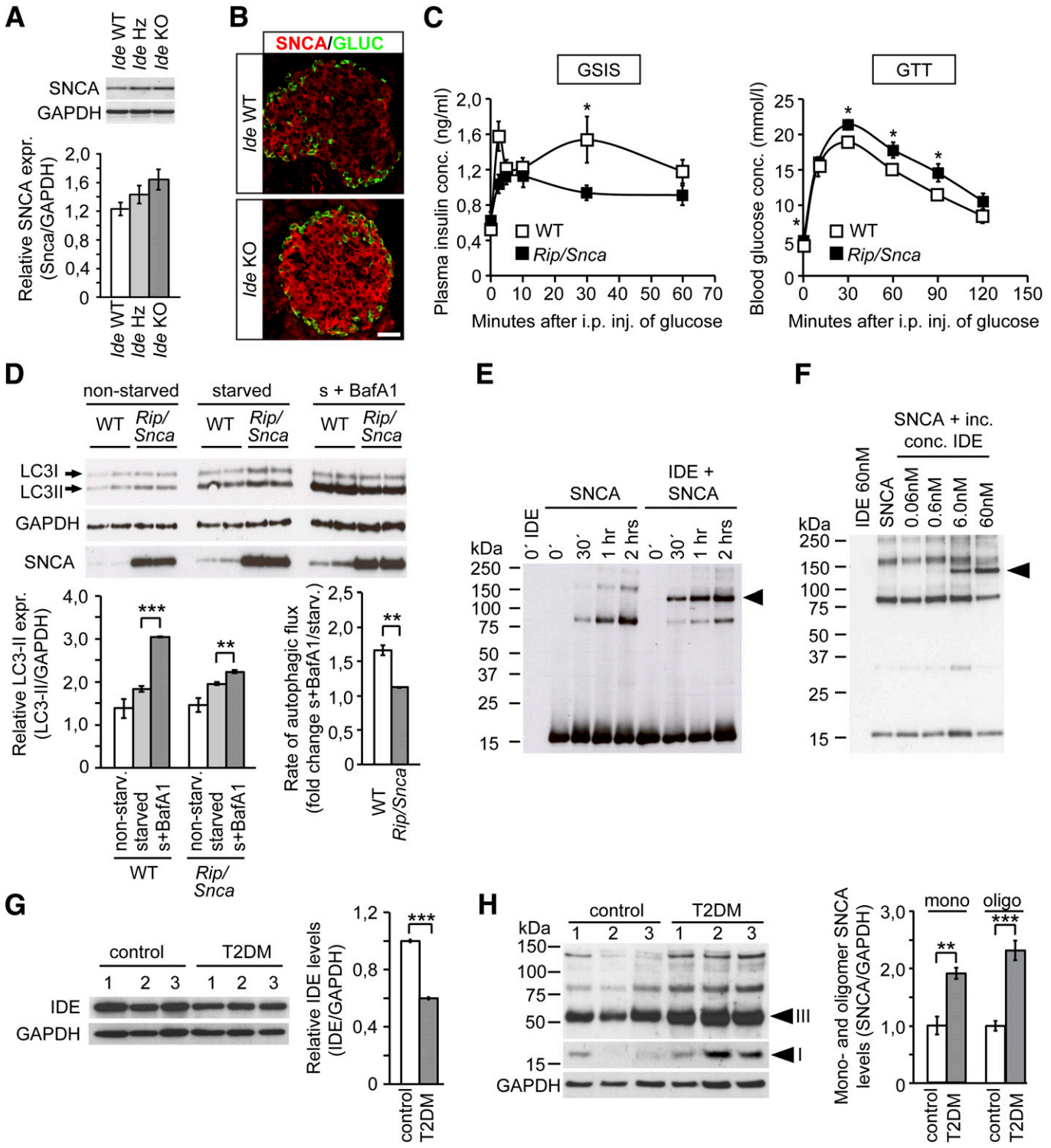

FIG. 5. α-Synuclein levels are increased in *Ide KO* islets. *A*: Immunoblot and quantification analyses of α-synuclein (SNCA) levels in isolated islets from *Ide* WT, *Ide* Hz, and *Ide* KO mice (n = 3 per genotype). *B*: Representative immunohistochemistry staining of *Ide* WT and *Ide* KO pancreas using SNCA (red) and glucagon (green) antibodies. Scale bar, 50 μm. *C*: GSIS and GTT performed on 10–17-week-old *Rip/Snca* (n = 11) and control (n = 9) mice. *D*: Immunoblot and quantification analyses of LC3-II and SNCA expression in nonstarved and starved ± BafA1 (s + BafA1) islets isolated from *Rip/Snca* (n = 6) and control (n = 6) mice. *E*: Representative immunoblot of SNCA incubated for 0', 30', 1 h, or 2 h in the absence or presence of recombinant IDE, using α-synuclein antibody. *F*: Representative immunoblot of SNCA incubated with increasing concentrations of recombinant IDE, using SNCA antibody. *G*: Representative immunoblot and quantification analyses of islets from T2D (n = 4) and nondiabetic (n = 4) patients using IDE antibody. *H*: Representative immunoblot and quantification analyses of islets from T2D and nondiabetic patients using SNCA antibody. Arrowheads indicate monomeric α-synuclein (I) and an ~50–70 kDa oligomeric product (III) in T2D islets. Data are presented as mean ± SEM. *P < 0.05; **P < 0.01; ***P < 0.001 (Student t test). GAPDH, glyceraldehyde-3-phosphate dehydrogenase.

IDE levels were decreased (by ~40%) in human T2D islets compared with nondiabetic controls (Fig. 5*G*). α-Synuclein monomeric levels were very low and in some cases barely detectable in islets from nondiabetic controls (Fig. 5*H*). Levels of α-synuclein monomers were, however, increased (by ~100%) in islets from T2D patients (Fig. 5*H*). In addition, an ~50–60-kD protein, or protein complex, recognized by α-synuclein antibodies was increased (by ~130%) in T2D islets compared with nondiabetic islets (Fig. 5*H*). Taken together, these findings provide evidence that levels of α-synuclein are inversely correlated with IDE levels in islets of *Ide*-deficient mice and human T2D patients.

To functionally assess whether the increase in levels of α-synuclein alone accounts for the impaired β-cell function of *Ide*-deficient mice, we bred the *Snca* KO allele onto the *Ide* KO background. Glucose tolerance tests (GTTs) showed that lack of *Snca* not only failed to rescue the impaired β-cell function of *Ide* mutant mice but insulin secretion was further blunted in *Ide* KO; *Snca* KO double mutant mice as compared with *Ide* KO mice (Fig. 6*A* and *B*). These data imply a role for *Snca* in GSIS, and GTTs revealed that *Snca* KO mice were glucose intolerant and had a severely impaired GSIS (Fig. 6*C* and *D*). Similarly, autophagic flux was reduced in islets of *Snca* KO mice (Fig. 6*F*) and worsened in *Ide*;*Snca* double KO islets as compared with *Ide* KO islets (Fig. 6*E*). Together these data not only show that loss of *Snca* in *Ide* KO mutant mice fails to rescue both the GSIS and autophagic flux phenotype in these mice but also suggest that *Snca*, in a dose-dependent manner, is required for normal GSIS and glucose tolerance as well as β-cell autophagy.

DISCUSSION

Our study shows that *Ide* controls β-cell function; mice lacking a functional *Ide* gene are hyperglycemic, glucose intolerant, and insulin secretion deficient due to reduced replenishment of the releasable pool of insulin granules. Farris et al. (9) and Abdul-Hay et al. (10) found that *Ide* KO mice were glucose intolerant, had increased fasting insulin levels, and showed evidence of insulin resistance and impaired insulin degradation, whereas Miller et al. (11) reported that *Ide* KO mice had normal glucose and insulin levels 4 h after refeeding of overnight-fasted mice. We do not find fasting insulin levels to be significantly elevated in *Ide* KO mice, nor do we find evidence of insulin resistance. Whether the differences in phenotype reflect differences in genetic background and/or methodologies used is unclear but underscores the still unresolved question regarding the role for IDE in insulin degradation (36). Nonetheless, we do find that *Ide* KO mice have significantly impaired GSIS, which was not explored in any of the other studies (9–11). We also find that the *Ide* gene is haploinsufficient and that IDE levels are inversely correlated with α-synuclein levels in mouse and human islets. Moreover, we show that increased levels of α-synuclein in β-cells impair GSIS and autophagy in vivo, and that IDE can form stable complexes with α-synuclein. These findings are *1*) consistent with the decreased insulin secretion associated with the *HHEX/IDE* T2D locus in humans (5,6,16), *2*) identify *Ide* as a key β-cell gene in vivo, thus implicating *IDE* as a potential T2D susceptibility allele, and *3*) suggest a mechanism for this risk allele in insulin secretion and diabetes in humans. These findings do not, however, rule out other role(s) for *Ide* in β-cells. Likewise, although our in vitro analyses are supportive of a cell-autonomous role for *Ide* in β-cells, the *Ide* KO mice analyzed in this study are global KOs; thus, we cannot exclude that the β-cell defect displayed by these mutants, at least in part, may be influenced by *Ide*-related deficiencies in other cells and tissues.

Our findings that GSIS is reduced in mice overexpressing α-synuclein in β-cells are supportive of previous data showing that overexpression of α-synuclein in an insulinoma cell line reduces basal, and to a lesser extent glucose-stimulated, insulin secretion (31). Together, these findings suggest that α-synuclein suppresses insulin secretion. Increased α-synuclein levels have been shown to negatively influence microtubule polymerization and trafficking (33,34), and a role for microtubules is implicated both in GSIS (27) and autophagy (28,29). Thus, the decreased microtubule content in both *Ide* and *Rip/Snca* islets suggests that the reduced GSIS and autophagy observed in these mice, at least in part, may result from negative effects of α-synuclein on microtubule polymerization and function. The exact role, if any, for microtubules in GSIS is however unclear; numerous studies implicate a role for microtubules in GSIS, in particular for the recruitment of granules for sustained insulin secretion (reviewed in 27), whereas others provide evidence against a role for microtubules in GSIS (26). α-Synuclein has been shown to interact with Kir6.2 at insulin granules (31) and overexpression of α-synuclein in vitro, possibly by negatively affecting Rab1a function, impairs growth hormone secretion and autophagy in mammalian cells (32), providing additional, microtubule-independent, mechanistic implications of increased levels of α-synuclein (Fig. 7).

Surprisingly, our analyses of *Snca* KO and *Ide* KO;*Snca* KO double mutant mice are supportive of a positive role for α-synuclein in β-cells; *Snca* KO mice showed severely reduced GSIS and attenuated autophagic flux in islets, and lack of *Snca* on an *Ide* KO background resulted in a further deterioration of GSIS and autophagy. In contrast, previous studies of in vitro glucose stimulation of α-synuclein–deficient islets showed evidence of an increased insulin secretion rate at low and medium, but not high, glucose levels (31). Whether the discrepancy between these findings reflects the in vitro versus in vivo experimental design is unclear but underscores the need for additional studies to address the mechanism by which *Snca* regulates insulin secretion. Notably, the exact physiological function of α-synuclein remains largely unknown but a role for α-synuclein in diverse processes like SNARE complex formation and mitochondrial calcium homeostasis has been suggested as has the idea that the toxic activities of α-synuclein may in fact reflect its normal function (37,38).

IDE has been shown to form stable, irreversible complexes with amyloidogenic proteins such as amyloidß (8), and our studies provide evidence that α-synuclein oligomerization is antagonized by this proposed "dead-end chaperone" activity of IDE in β-cells (Fig. 7). Human IAPP is also an IDE substrate, and in contrast to rodent IAPP, human IAPP can develop toxic oligomers and amyloid deposits, which are commonly observed in β-cells of T2D patients (39,40). In humans, reduced IDE expression and/or activity may thus lead to increased levels of IAPP oligomers and, with time, the formation of IAPP amyloid deposits and β-cell destruction. Autophagy is important for selective degradation of accumulated and aggregated proteins, sometimes referred to as aggrephagy (41). Thus, independent of IDE expression or activity, conditions leading to reduced autophagy in β-cells likely lead to

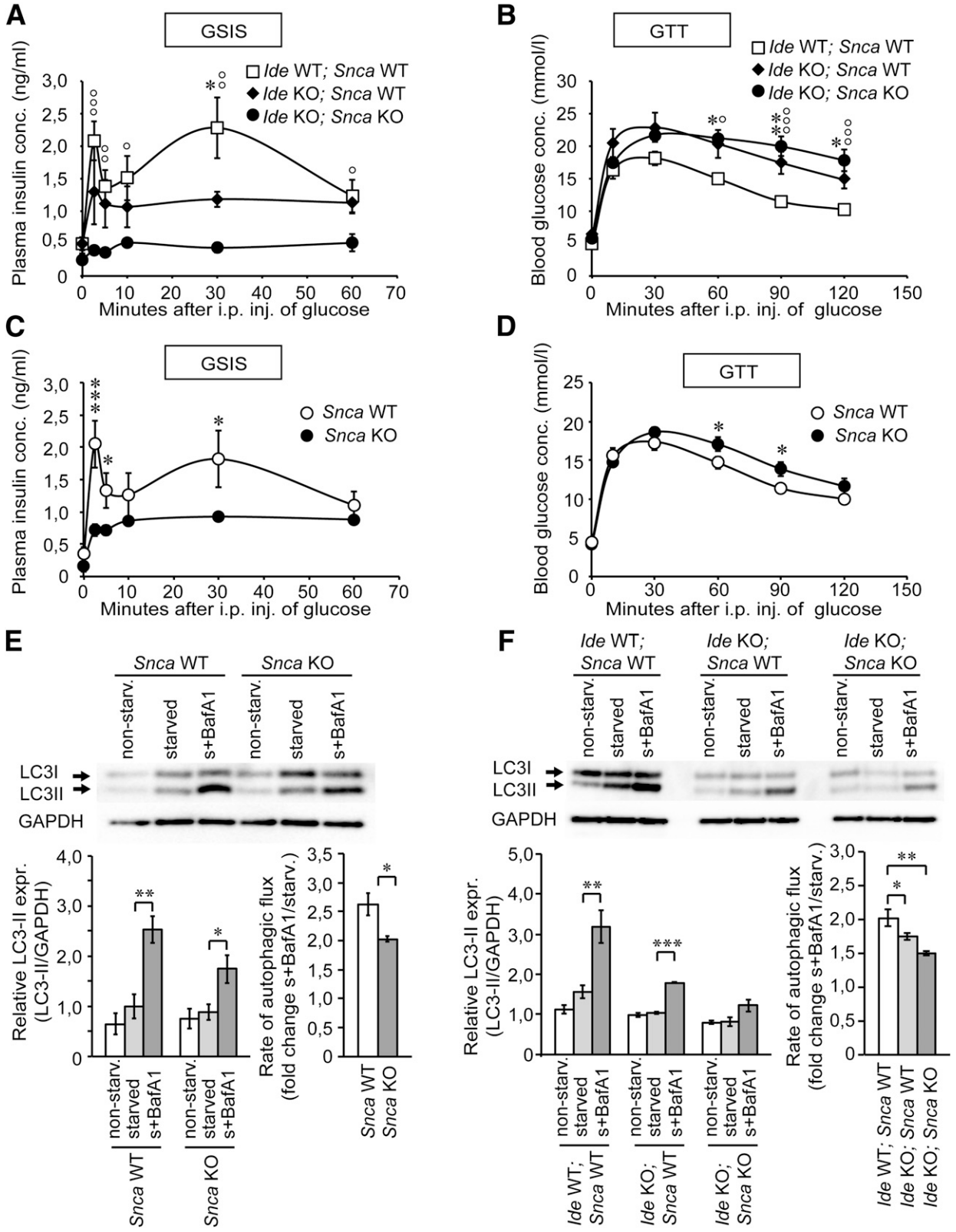

FIG. 6. α-Synuclein mutant (*Snca* KO) mice show decreased GSIS and reduced autophagy flux in islets. *A–D*: Insulin (*A* and *C*) and glucose (*B* and *D*) levels during GTT performed on 7–9-week-old *Ide* WT, *Ide* KO, *Snca* KO;*Ide* KO (*A* and *B*), *Snca* WT, and *Snca* KO mice (*C* and *D*) (n = 8–15 per genotype). Significance is indicated for comparison of datasets between *Ide* WT and *Ide* KO (*), *Snca* WT and *Snca* KO (*), and *Ide* WT and *Snca* KO;*Ide* KO (°), respectively. *E* and *F*: Immunoblot and quantification analyses of LC3-II expression in nonstarved and starved *Ide* WT, *Ide* KO, *Snca* KO;*Ide* KO, *Snca* KO, and *Snca* WT islets, in the absence or presence of BafA1 (s + BafA1) (n = 6 mice per genotype). Data are presented as mean ± SEM. *$P < 0.05$; **$P < 0.01$; ***$P < 0.001$ (Student t test). GAPDH, glyceraldehyde-3-phosphate dehydrogenase.

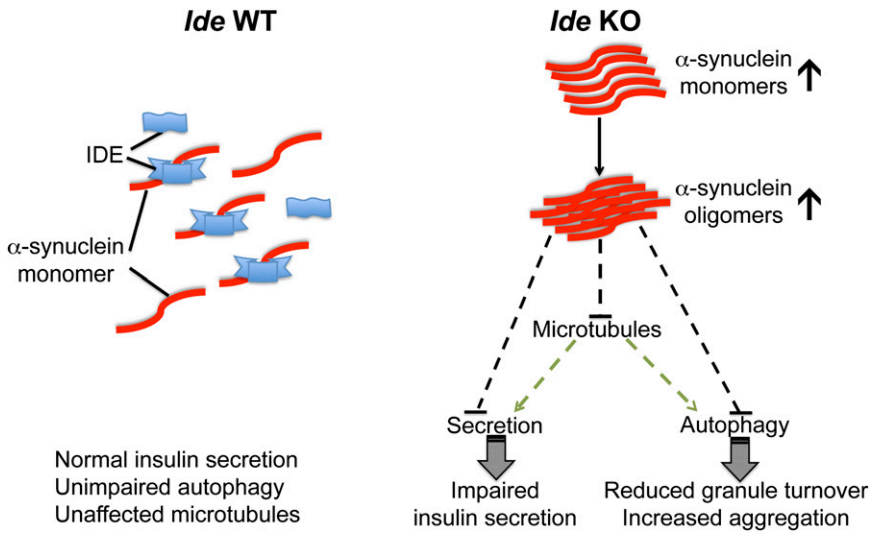

FIG. 7. Model for the role of IDE in β-cell function. IDE forms irreversible complexes with α-synuclein monomers. Loss of *Ide* in β-cells leads to increased levels of free α-synuclein monomers that, via subsequent formation of oligomers, impair insulin secretion and autophagy, possibly in part by attenuation of the microtubule network.

increased intracellular levels of not only α-synuclein but also IAPP oligomers and an enhanced likelihood of IAPP aggregation and consequently amyloid formation in human β-cells.

T2D is associated with both age and obesity, and IDE activity has been shown to decline with age (42) and be inhibited by long-chain free fatty acids (43). Moreover, autophagy is inhibited by insulin, and conditions leading to increased insulin levels, e.g., ageing and obesity, are associated with impaired autophagy (44). Hence, increasing age and obesity likely result in reduced IDE activity as well as autophagy and consequently decreased turnover and/or neutralization of amyloidogenic proteins such as α-synuclein and IAPP, which in turn may lead to β-cell degeneration. Thus, stimulation of IDE expression or activity could represent a valuable therapeutic strategy for the prevention and/or restoration of β-cell function in T2D patients.

ACKNOWLEDGMENTS

This work was supported by grants from the Swedish Research Council, the Strategic Research Program in Diabetes at Umeå University, the Wallenberg Foundation, the European Union (Integrated Project EuroDia LSHM-CT-2006-518153 in the Framework Program 6 of the European Community), the Kempe Foundation, the Swedish Diabetes Association, and the Novo Nordisk Foundation (to H.E.).

H.E. is a cofounder, shareholder, and consultant of the unlisted biotech company Betagenon. C.-G.Ö. is on the advisory boards of Novo Nordisk and Eli Lilly and is a shareholder of the Swedish biotech company Orexo. No other potential conflicts of interest relevant to this article were reported.

P.S. designed and performed in vivo analyses of the control, HFD-fed, aged, and transgenic mice, as well as in vitro islet culture; interpreted results; helped write the paper; and determined insulin, amylin, and glucagon pancreatic content. L.B. performed WB analyses, tubulin and actin fractionations, autophagic flux analyses, and protein aggregation and degradation assays and helped write the paper. S.E. assisted with immunofluorescence studies, cell counting, and mRNA expression analyses. L.L. performed WB analyses, tubulin and actin fractionations, autophagic flux analyses, and protein aggregation and degradation assays. F.B. prepared mouse islets and performed islet perifusion analyses. C.-G.Ö. provided human islets. H.E. designed and supervised the study, analyzed and interpreted the data, and wrote the paper. H.E. is the guarantor of this work and, as such, had full access to all the data in the study and takes responsibility for the integrity of the data and the accuracy of the data analysis.

Parts of this study were presented as an oral presentation at the Korea-Sweden Symposium on Frontier Sciences, Seoul, Korea, 30–31 May 2012.

The authors thank members of their laboratory for technical instructions, suggestions, and helpful discussions; Dr. Malcolm A. Leissring (Mayo Clinic, Jacksonville, Florida) for the generous gift of IDE 6A1 mAb; and Drs. Thomas Edlund and Sara Wilson (Umeå University) for critical reading and help in the preparation of the manuscript.

REFERENCES

1. Perry JR, Frayling TM. New gene variants alter type 2 diabetes risk predominantly through reduced beta-cell function. Curr Opin Clin Nutr Metab Care 2008;11:371–377
2. Saxena R, Voight BF, Lyssenko V, et al.; Diabetes Genetics Initiative of Broad Institute of Harvard and MIT, Lund University, and Novartis Institutes of BioMedical Research. Genome-wide association analysis identifies loci for type 2 diabetes and triglyceride levels. Science 2007;316:1331–1336
3. Scott LJ, Mohlke KL, Bonnycastle LL, et al. A genome-wide association study of type 2 diabetes in Finns detects multiple susceptibility variants. Science 2007;316:1341–1345
4. Zeggini E, Weedon MN, Lindgren CM, et al.; Wellcome Trust Case Control Consortium (WTCCC). Replication of genome-wide association signals in UK samples reveals risk loci for type 2 diabetes. Science 2007;316:1336–1341
5. Grarup N, Rose CS, Andersson EA, et al. Studies of association of variants near the HHEX, CDKN2A/B, and IGF2BP2 genes with type 2 diabetes and impaired insulin release in 10,705 Danish subjects: validation and extension of genome-wide association studies. Diabetes 2007;56:3105–3111
6. Pascoe L, Tura A, Patel SK, et al.; RISC Consortium; U.K. Type 2 Diabetes Genetics Consortium. Common variants of the novel type 2 diabetes genes

CDKAL1 and HHEX/IDE are associated with decreased pancreatic beta-cell function. Diabetes 2007;56:3101–3104
7. Kurochkin IV. Insulin-degrading enzyme: embarking on amyloid destruction. Trends Biochem Sci 2001;26:421–425
8. Llovera RE, de Tullio M, Alonso LG, et al. The catalytic domain of insulin-degrading enzyme forms a denaturant-resistant complex with amyloid beta peptide: implications for Alzheimer disease pathogenesis. J Biol Chem 2008;283:17039–17048
9. Farris W, Mansourian S, Chang Y, et al. Insulin-degrading enzyme regulates the levels of insulin, amyloid beta-protein, and the beta-amyloid precursor protein intracellular domain in vivo. Proc Natl Acad Sci USA 2003;100:4162–4167
10. Abdul-Hay SO, Kang D, McBride M, Li L, Zhao J, Leissring MA. Deletion of insulin-degrading enzyme elicits antipodal, age-dependent effects on glucose and insulin tolerance. PLoS ONE 2011;6:e20818
11. Miller BC, Eckman EA, Sambamurti K, et al. Amyloid-beta peptide levels in brain are inversely correlated with insulysin activity levels in vivo. Proc Natl Acad Sci USA 2003;100:6221–6226
12. Zambrowicz BP, Friedrich GA, Buxton EC, Lilleberg SL, Person C, Sands AT. Disruption and sequence identification of 2,000 genes in mouse embryonic stem cells. Nature 1998;392:608–611
13. Edfalk S, Steneberg P, Edlund H. Gpr40 is expressed in enteroendocrine cells and mediates free fatty acid stimulation of incretin secretion. Diabetes 2008;57:2280–2287
14. Steneberg P, Rubins N, Bartoov-Shifman R, Walker MD, Edlund H. The FFA receptor GPR40 links hyperinsulinemia, hepatic steatosis, and impaired glucose homeostasis in mouse. Cell Metab 2005;1:245–258
15. Ostenson CG, Gaisano H, Sheu L, Tibell A, Bartfai T. Impaired gene and protein expression of exocytotic soluble N-ethylmaleimide attachment protein receptor complex proteins in pancreatic islets of type 2 diabetic patients. Diabetes 2006;55:435–440
16. Rudovich N, Pivovarova O, Fisher E, et al. Polymorphisms within insulin-degrading enzyme (IDE) gene determine insulin metabolism and risk of type 2 diabetes. J Mol Med (Berl) 2009;87:1145–1151
17. Halban PA, Wollheim CB. Intracellular degradation of insulin stores by rat pancreatic islets in vitro. An alternative pathway for homeostasis of pancreatic insulin content. J Biol Chem 1980;255:6003–6006
18. Uchizono Y, Alarcón C, Wicksteed BL, Marsh BJ, Rhodes CJ. The balance between proinsulin biosynthesis and insulin secretion: where can imbalance lead? Diabetes Obes Metab 2007;9(Suppl. 2):56–66
19. Mizushima N, Yoshimori T, Levine B. Methods in mammalian autophagy research. Cell 2010;140:313–326
20. Huopio H, Shyng SL, Otonkoski T, Nichols CG. K(ATP) channels and insulin secretion disorders. Am J Physiol Endocrinol Metab 2002;283:E207–E216
21. Thams P, Capito K. L-arginine stimulation of glucose-induced insulin secretion through membrane depolarization and independent of nitric oxide. Eur J Endocrinol 1999;140:87–93
22. Garcia MC, Hermans MP, Henquin JC. Glucose-, calcium- and concentration-dependence of acetylcholine stimulation of insulin release and ionic fluxes in mouse islets. Biochem J 1988;254:211–218
23. Yaekura K, Julyan R, Wicksteed BL, et al. Insulin secretory deficiency and glucose intolerance in Rab3A null mice. J Biol Chem 2003;278:9715–9721
24. Gunawardana SC, Liu YJ, Macdonald MJ, Straub SG, Sharp GW. Anaplerotic input is sufficient to induce time-dependent potentiation of insulin release in rat pancreatic islets. Am J Physiol Endocrinol Metab 2004;287:E828–E833
25. Mourad NI, Nenquin M, Henquin JC. Metabolic amplifying pathway increases both phases of insulin secretion independently of beta-cell actin microfilaments. Am J Physiol Cell Physiol 2010;299:C389–C398
26. Mourad NI, Nenquin M, Henquin JC. Metabolic amplification of insulin secretion by glucose is independent of β-cell microtubules. Am J Physiol Cell Physiol 2011;300:C697–C706
27. Wang ZX, Thurmond DC. Mechanisms of biphasic insulin-granule exocytosis - roles of the cytoskeleton, small GTPases and SNARE proteins. J Cell Sci 2009;122:893–903
28. Fass E, Shvets E, Degani I, Hirschberg K, Elazar Z. Microtubules support production of starvation-induced autophagosomes but not their targeting and fusion with lysosomes. J Biol Chem 2006;281:36303–36316
29. Köchl R, Hu XW, Chan EYW, Tooze SA. Microtubules facilitate autophagosome formation and fusion of autophagosomes with endosomes. Traffic 2006;7:129–145
30. Pipeleers DG, Pipeleers-Marichal MA, Kipnis DM. Microtubule assembly and the intracellular transport of secretory granules in pancreatic islets. Science 1976;191:88–90
31. Geng X, Lou H, Wang J, et al. α-Synuclein binds the K(ATP) channel at insulin-secretory granules and inhibits insulin secretion. Am J Physiol Endocrinol Metab 2011;300:E276–E286
32. Winslow AR, Chen CW, Corrochano S, et al. α-Synuclein impairs macroautophagy: implications for Parkinson's disease. J Cell Biol 2010;190:1023–1037
33. Chen L, Jin J, Davis J, et al. Oligomeric alpha-synuclein inhibits tubulin polymerization. Biochem Biophys Res Commun 2007;356:548–553
34. Lee HJ, Khoshaghideh F, Lee S, Lee SJ. Impairment of microtubule-dependent trafficking by overexpression of alpha-synuclein. Eur J Neurosci 2006;24:3153–3162
35. El-Agnaf OM, Irvine GB. Review: formation and properties of amyloid-like fibrils derived from alpha-synuclein and related proteins. J Struct Biol 2000;130:300–309
36. Roth R, Ding L, Becker A. Insulin degradation. In *Diabetes Mellitus: A Fundamental and Clinical Text*. LeRoith D, Taylor S, Olefsky J, Eds. Lippincott Williams & Wilkins, Philadelphia, PA, 2003
37. Burré J, Sharma M, Tsetsenis T, Buchman V, Etherton MR, Südhof TC. Alpha-synuclein promotes SNARE-complex assembly in vivo and in vitro. Science 2010;329:1663–1667
38. Cooper AA, Gitler AD, Cashikar A, et al. Alpha-synuclein blocks ER-Golgi traffic and Rab1 rescues neuron loss in Parkinson's models. Science 2006;313:324–328
39. Clark A, Nilsson MR. Islet amyloid: a complication of islet dysfunction or an aetiological factor in type 2 diabetes? Diabetologia 2004;47:157–169
40. Haataja L, Gurlo T, Huang CJ, Butler PC. Islet amyloid in type 2 diabetes, and the toxic oligomer hypothesis. Endocr Rev 2008;29:303–316
41. Yamamoto A, Simonsen A. The elimination of accumulated and aggregated proteins: a role for aggrephagy in neurodegeneration. Neurobiol Dis 2011;43:17–28
42. Runyan K, Duckworth WC, Kitabchi AE, Huff G. The effect of age on insulin-degrading activity in rat tissue. Diabetes 1979;28:324–325
43. Hamel FG, Upward JL, Bennett RG. In vitro inhibition of insulin-degrading enzyme by long-chain fatty acids and their coenzyme A thioesters. Endocrinology 2003;144:2404–2408
44. Mizushima N, Levine B, Cuervo AM, Klionsky DJ. Autophagy fights disease through cellular self-digestion. Nature 2008;451:1069–1075